Diffusion-based Physical Channel Identification in Molecular Nanonetworks

Nora Garralda[a], Ignacio Llatser[a,*], Albert Cabellos-Aparicio[a], Eduard Alarcón[a], Massimiliano Pierobon[b]

[a] *Nanonetworking Center in Catalonia (N3Cat), Universitat Politècnica de Catalunya, c/Jordi Girona, 1-3, 08034 Barcelona, Spain*
[b] *Broadband Wireless Networking (BWN) Laboratory, School of Electrical and Computer Engineering, Georgia Institute of Technology, 250 14th Street, Atlanta, GA 30332, United States*

Abstract

Nanonetworking is an emerging field of research at the intersection of nanotechnology and communication networks. Molecular Communication (MC) is a bio-inspired paradigm, where nanonetworks, i.e., the interconnection of nanodevices, are implemented based on the exchange of molecules. Within this paradigm, one of the most promising techniques is diffusion-based MC, which relies on free diffusion to transport the molecules from transmitter to receiver. We explore in this work the main characteristics of diffusion-based MC through the use of *N3Sim*, a physical simulation framework for MC which allows the simulation of the physics underlying the diffusion of molecules in different scenarios. Through the results obtained with *N3Sim*, the Linear Time Invariant (LTI) property is proven to be a valid assumption for the normal diffusion-based MC scenario. Moreover, diffusion-based noise is observed and evaluated with reference to existing stochastic models. Furthermore, the optimal pulse shape for diffusion-based MC is found to be a narrow spike. Finally, four different pulse-based coding techniques are compared in terms of available bandwidth, ISI and energy consumption for communication; On-Off Keying is found to be the most suitable scheme

*Corresponding author. Tel.: +34 934017182; fax: +34 934017055.
Email addresses: garralda@ac.upc.edu (Nora Garralda), llatser@ac.upc.edu (Ignacio Llatser), acabello@ac.upc.edu (Albert Cabellos-Aparicio), ealarcon@eel.upc.edu (Eduard Alarcón), maxp@ece.gatech.edu (Massimiliano Pierobon)

in the evaluated scenario.

Keywords: Nanonetworks, Diffusion-based Molecular Communication, Channel Identification, Diffusion

1. Introduction

Nanotechnology, the study of nanometer-scale systems, is a multidisciplinary research area with potential applications in the biomedical, environmental and industrial field [1]. A nanomachine is the most basic functional unit able to perform very simple tasks at the nanoscale, including computing, data storage, sensing, actuation and communication.

Nanonetworks, the interconnection of nanomachines, have emerged as a novel research field which has attracted the interest of researchers from the domains of information and communication technology, nanotechnology and biology. Nanonetworks will provide means for cooperation and information sharing among nanomachines, allowing them to fulfill more complex tasks. Several alternative methods have been proposed to interconnect nanomachines, leading to a novel paradigm to implement communications at the nanoscale: Molecular Communication (MC) [1]. MC enables the interconnection of nanomachines through the exchange of molecules. MC spans several different communication solutions according to the way molecules are propagated and they are classified in relation to the communication range. For short distances, (nm-μm), molecular motors [2] and calcium signaling have been proposed [3, 4]; for the medium range (μm-mm), the use of the flagellated bacteria and catalytic nanomotors [5] has been studied and simulated; for the long range (mm-m), communication by means of pheromones has been suggested [6] as a possible solution.

This work is focused on diffusion-based MC [7], where transmitters suspended in a fluid medium emit molecules according to a release pattern which encodes the transmitted information. The emitted molecules move following an erratic trajectory, due to the collisions between them and the molecules of the fluid. As a consequence of this movement and of interactions among the emitted molecules (such as collisions and electrostatic forces), the emitted molecules diffuse throughout the medium. This diffusion causes the concentration of molecules to propagate and spread throughout the space. Finally, receivers measure the local concentration of molecules at their neighborhood and decode the transmitted information.

Diffusion-based MC, and the resulting molecular nanonetworks, are especially aimed to intra-body scenarios due to their low power requirements and high biocompatibility. Potential applications of molecular nanonetworks include, but are not limited to, intelligent drug delivery systems, diagnostic and therapeutic antiviral activities, and prosthetic implants techniques [8, 9, 10].

Several research efforts have been focused on the physical modeling of the channel in diffusion-based MC. As an example, physical models for the channel as well as bio-inspired transmitters and receivers are provided in [7]. Information-theoretical approaches which compute the channel capacity have also been applied in [11, 12, 13, 14]. We believe that in order to validate these models and provide a common ground to compare them, tests either by means of simulation or experimentation should be provided.

The work presented in this paper is focused on the study of the diffusion-based MC channel by using the simulation framework *N3Sim*. Through *N3Sim* we are able to simulate the physics underlying the propagation of molecules in different MC scenarios. As a result, we obtain several parameters related to the communication characteristics of the diffusion-based MC channel, such as the attenuation, the delay and the noise features. *N3Sim* enables also the comparison between different modulation schemes for diffusion-based MC.

The remainder of this paper is organized as follows. In Section 2, we introduce the physical layer simulator for the diffusion-based molecular channel, *N3Sim*. In Section 3, we review the different diffusion scenarios related to the assumptions on the physical behavior of the molecules. In Section 4, we examine the noise in a molecular channel and we validate it by simulation. In Section 5, we prove that the diffusion-based MC channel is linear and time-invariant. In Section 6, we identify the normal diffusion-based channel with a finite impulse response and a channel transfer function. In Section 7, we show the effects of changing the shape and length of the transmitted pulses of concentration. Next, in Section 8, we evaluate several modulation techniques and we find the optimal scheme in terms of communication performance. Finally, Section 9 concludes the paper.

2. Overview of N3Sim

N3Sim is a simulation framework for the general case of diffusion-based MC, which simulates the diffusion-based molecular channel according to the Brownian dynamics of the molecules in a fluid medium. Through *N3Sim*,

we also simulate interactions among the molecules, such as elastic collisions, when molecules exchange kinetic energy, or electrostatic interactions that appear when the molecules have an electrical charge. As an extension of the Brownian motion, *N3Sim* simulates also the correlated random walk.

The user can edit multiple parameters, such as the number of transmitters/receivers (as well as their locations), the radius of emitted molecules, the emission pattern for each transmitter, the fluid viscosity and the diffusion coefficient, and a bounded/unbounded space, amongst others.

Through *N3Sim*, a user may choose how the transmitter encodes the information: i) into the number of emitted molecules, known as information molecules, or ii) into the molecule concentration at the transmitter location. Furthermore, receivers estimate the local concentration by counting the number of molecules within their sensing area over time. The user may also choose between two types of receiver: i) an ideal receiver transparent to the diffusion process, and ii) a receiver that absorbs the molecules after they enter its actuation area.

The benefits of *N3Sim* with respect to other diffusion-based MC simulators, such as [15], come from the fact that it simulates the motion of every single molecule independently, which allows for the observation of the effect of the molecules interactions and the uncertainty introduced by the Brownian motion. Moreover, *N3Sim* allows the simulation of scenarios having virtually any number of transmitters and receivers. This feature enables simulations where the molecular information is broadcast from one transmitter to many receivers, or where more than one transmitter access the channel at the same time.

More details about *N3Sim*, along with its freely available source code, may be found in the website of the Nanonetworking Center in Catalunya (`http://www.n3cat.upc.edu/n3sim`).

3. Molecular Diffusion Simulation Scenarios

The diffusion process is defined as the spontaneous spread of molecules throughout space due to a gradient in the concentration of molecules. This process tends towards the homogenization of the molecule concentration in the fluid medium, causing a net flux of molecules from zones with higher concentration to the lower concentration zones [16].

The diffusion process is mathematically modeled by the Fick's laws of diffusion for the case of having a moderate concentration of molecules, so that

each molecule motion can be considered as independent [17]. Brownian motion is the continuous-time stochastic process which underlies diffusion, and it is observed in a microscopic scale as the jittery motion that the molecules show upon collision with other neighboring molecules.

Brownian dynamics defines the mean square displacement of a molecule subject to diffusion, in each direction, as $\langle x \rangle^2 = 2Dt^\alpha$. D is the diffusion coefficient, defined for spherical molecules whose mass and size are much larger than those of the medium in which they are floating. This case corresponds to low Reynolds number conditions [18], which means that viscous forces dominate the process. When the mean square displacement is directly proportional to time, $\alpha = 1$, then the resulting process is called normal diffusion. This scenario, can be simulated through *N3Sim*, which models the motion of every single molecule following the Brownian dynamics, and the results are validated by comparison to the Fick's laws of diffusion.

When $\alpha < 1$ or $\alpha > 1$, the resulting process is called anomalous diffusion. Collective diffusion is a case of anomalous diffusion and it occurs when there is a very high concentration of molecules. Due to the large amount of molecules, the interactions between them impact the diffusion process, which can no longer be modeled with the Fick's laws of diffusion.

The mathematical process underlying anomalous diffusion is the correlated random walk, a Lèvy process [19] which includes memory. This contrasts with the Brownian motion, whose main feature is the absence of time correlation, thus being a memoryless process. Correlated random walk is a discrete version of the Brownian motion, that spans the whole range of random walks, from ballistic to dispersal motions [20], where molecules always experience the same step size and they change their direction with a certain probability. The macroscopic view of the correlated random walk is modeled by the hyperbolic diffusion equation.

N3Sim allows modeling collective diffusion by simulating a large number of molecules and by taking into account elastic collisions among them. The observed results are that, in the tested scenarios, collisions among the information molecules have the same effect as collisions among the information and the fluid molecules. As a result, in this scenario the Fick's laws are a valid model for the molecule diffusion. Nevertheless, if electrostatic interactions are taken into account, these forces dominate the particle motion, which is then much faster and more directed than in the free diffusion and the Fick's laws are not longer valid. Finally, by adding an initial velocity to the emitted molecules, as well as inertia, which is the property of a molecule

to remain at a constant velocity, *N3Sim* approximates the case of correlated random walk. The results for this case are validated by comparison to the hyperbolic diffusion equation solution [7].

4. Noise in Diffusion-based Molecular Communication

Brownian motion is a source of uncertainty in the space distribution of particles, and it causes the exact location of a particle to be unknown. As a consequence, even in a system with a homogeneous particle concentration, we cannot predict the exact number of particles within a space area.

When a receiver estimates the concentration by sensing the number of molecules within its actuation area over time, the uncertainty of Brownian motion is observed as a noise source, i.e., an unwanted perturbation on the received concentration signal. This effect has been modeled by means of a probabilistic model in [21], and it is called Particle Counting Noise. In this model, the number of particles N_p measured by a receiver follows a non-homogeneous Poisson counting process, whose rate of occurrence is equal to the concentration $c(t)$ of molecules: $N_p \sim Poiss(c(t))$

We have validated the diffusion noise through *N3Sim* by verifying that the number of particles in a space follows a non-homogeneous Poisson counting process, with the actual concentration as the rate of the process, by the comparison of two likelihood tests.

We consider a scenario with two different homogeneous concentrations of molecules over time. We first simulate the system with the lower concentration and after that we apply the higher one. We have created our data set by locating one hundred receivers all over the system that estimate the concentration independently. Each estimation shows unique values with respect to other estimation performed by other receivers in the same conditions. This is a consequence of the Particle Counting Noise.

In Fig. 1, we can see the result of two likelihood tests. The upper likelihood test shows how likely the number of measured molecules N_p is to follow a normal process with mean and variance equal to the actual concentration. The lower likelihood test shows how likely is N_p to follow a Poisson process with rate equal to the actual concentration. The mean value of the likelihood tests are 0.91 and 0.9923, respectively. As a consequence, the simulation results indicate that diffusion-based noise is better modeled by the Particle Counting Noise from [21].

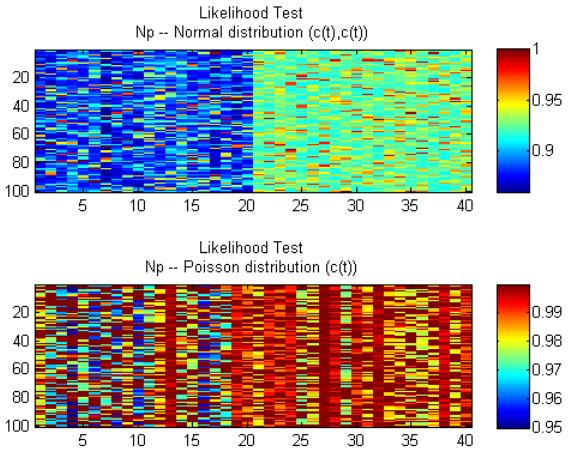

Figure 1: Normal and Poisson Likelihood tests comparison

This noise can be related to the shot noise in optical communications. Similarly to the shot noise, the Particle Counting Noise, is signal-dependent, i.e., the higher is the power of the transmitted signal, the higher is the power of the noise that affects the received signal.

5. Channel Linearity and Time Invariance

A Linear Time-Invariant (LTI) channel fulfills the superposition principle [22] and maintains its features over time. In order to verify whether the molecular diffusion-based channel has the LTI property, we have considered the most regular scenario, the normal diffusion process, and we have distinguished two cases: the *single-transmitter scenario* and the *multi-transmitter scenario*. We analyze them in the following:

5.1. Single-transmitter scenario

In Fig. 2, the superposition principle is verified. The upper image shows three different transmitted signals: a Gaussian pulse ($x1$), a square pulse ($x2$), and the addition of both pulses ($y = x1 + x2$). The lower image shows the reception of these pulses at a certain distance, as well as the colored area which is the sum of the outputs as if their corresponding inputs where applied independently with respect to the channels. As it is shown in Fig. 2,

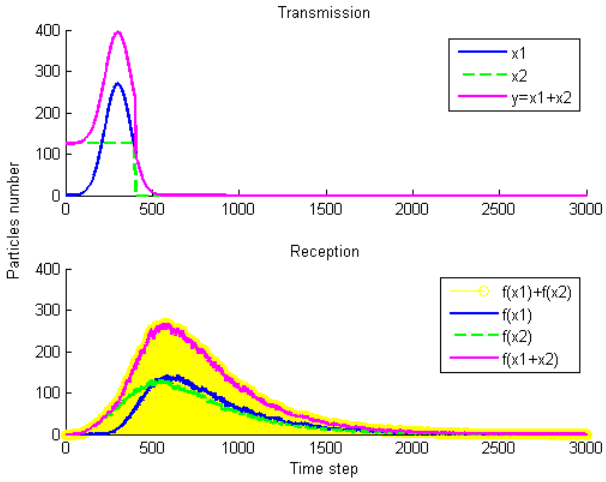

Figure 2: Linearity validation for the single user scenario by verifying the homogeneity and additive properties. Transmission and reception of a Gaussian pulse, a square pulse and the addition of both.

the colored area matches with the output of the sum of the transmitted signals. These results should confirm the linearity of the channel.

The upper image of Fig. 3 shows the transmitted signals, two Gaussian pulses, one delayed with respect to the other, $(x[n], x[n-100])$. The lower image of Fig. 3 shows the reception of the pulses, and how the delay between the outputs matches with the delay between the corresponding inputs. As a consequence, the channel behaves as time-invariant.

5.2. Multi-transmitter scenario

For the muti-transmitter scenario we consider in this analysis the case of having two independent transmitters. To validate the LTI property, first, transmitter A transmits a pulse, and after that, a second transmitter B transmits another pulse. When both pulses are transmitted at the same time, we check whether an equidistant receiver measures the same signal power as the sum of the two outputs corresponding to single pulses transmitted independently

In Fig. 4, the superposition principle is validated. We observe in the upper image the transmission of two different signals from transmitters A and B, a square pulse $(x1)$, and a spike of particles $(x2)$ as the narrowest possible pulse emitted, both containing the same energy. The lower image shows the

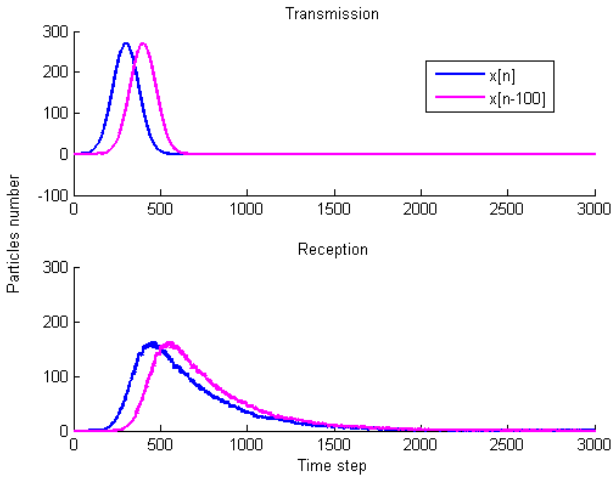

Figure 3: Temporal invariance validation for the single-transmitter scenario. Transmission and reception of two Gaussian pulses in different times.

reception by a receiver 500 nm away from both transmitters, ($f(x1)$,$f(x2)$), as well as the reception of the simultaneous transmission of the two pulses ($f(x1+x2)$). Finally, the colored area shows the sum of the two independent transmissions ($f(x1) + f(x2)$). This area matches with the received signal corresponding to the emission of both pulses simultaneously, thus confirming that the channel shows the linearity property also for the multi-transmitter case.

In Fig. 5, we observe that the channel is time-invariant also for the multi-transmitter case. The upper image shows both transmitters, A and B, transmitting a square pulse in different time instants, ($x1$, $x2$). The lower image shows the reception of each transmission, ($f(x1)$, $f(x2)$) at a distance of 500 nm from the transmitters, and the received signal when both transmitters are transmitting simultaneously ($f(x1 + x2)$). Again, we conclude that the delay among the transmitted pulses is the same whether or not they are transmitted simultaneously.

In conclusion, we have obtained that the channel satisfies both conditions of linearity and time invariance for both scenarios, the single-transmitter scenario and the multi-transmitter scenario. This means that when different transmitters transmit the same type of particles, the interactions among them are negligible and the channel can be modeled through the Fick's laws of diffusion.

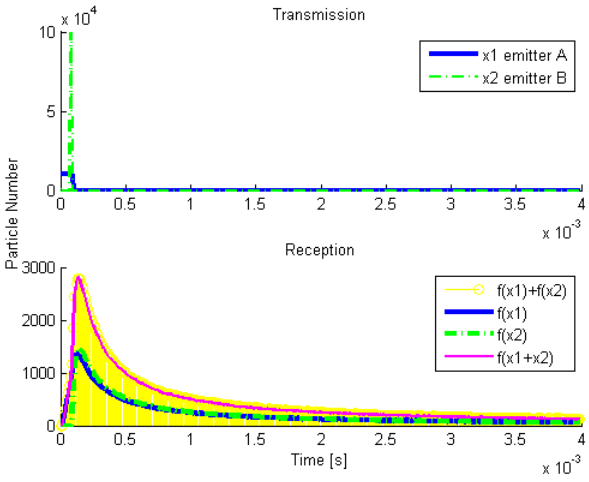

Figure 4: Linearity validation for the multi-user scenario by verifying the homogeneity and additive properties. Transmission and reception of two square pulses, one wider than the other but with the same transmitted energy.

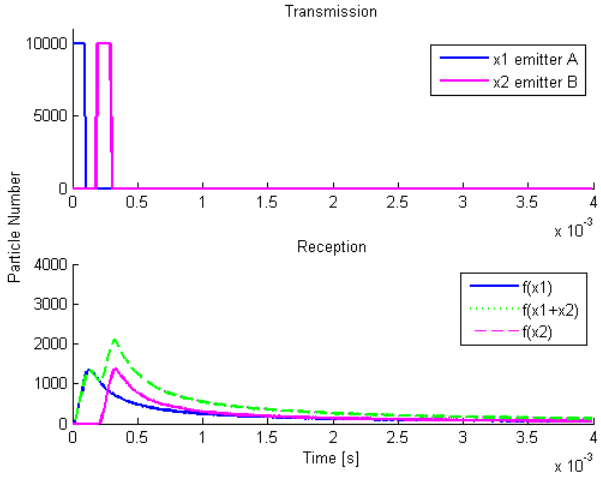

Figure 5: Temporal invariance validation for the multi-user scenario. Transmission and reception of two square pulses from different emitters, in different times.

The operation range of nanomachines is limited by the energy of the transmitted pulses or, equivalently, the total number of emitted particles. Since we have observed that the channel is LTI, the effect of one transmitter releasing a certain number of particles to the medium is equivalent to two transmitters, each releasing half of this quantity. Therefore, by adding emitters that transmit coordinately we can extend the range of the transmitted signal.

If different emitters use different types of particles and the interactions among them are negligible, the channel capacity can also be increased by creating independent channels, e.g., by using the *Molecular Division Multiple Access* technique proposed in [6].

6. Diffusion-based Channel Identification

The Linear Time Invariant property is proven to be a valid assumption for the normal diffusion-based MC scenario; hence, the expression for the Finite Impulse Response (FIR) as a function of distance embodies all significant characteristic features of the channel.

In a diffusion-based MC channel, the information molecules released by a nanomachine physically move according to Brownian dynamics. The propagation mean delay increases with the square of the transmission distance [23]; therefore, a degradation of the capacity for this channel when increase of the transmission distance is expected. The normal diffusion process is mainly characterized by the diffusion coefficient D which determines how fast the diffusion is and includes all the information from the environment.

By means of a simulation-based analysis, we have obtained the impulse responses for a range of distances between the transmitter and the receiver. The obtained results fit with the solution of the Second Fick's Law of diffusion, which describes the statistical properties of the spatial and temporal evolution that a concentration of particles exhibits under the same boundary and initial conditions.

Fig. 6 shows the impulse response of the diffusion-based MC channel obtained for calcium particles ($r = 0.2nm$) immersed in cytoplasm fluid in a 3-dimensional space for a set of transmission distances in the range of 0–1 μm. We observe that the width of the impulse response increases with the transmission distance. In consequence, the available bandwidth will decrease with the distance and any transmitted concentration sequence will suffer a distortion in shape, resulting in a widening of the received signal.

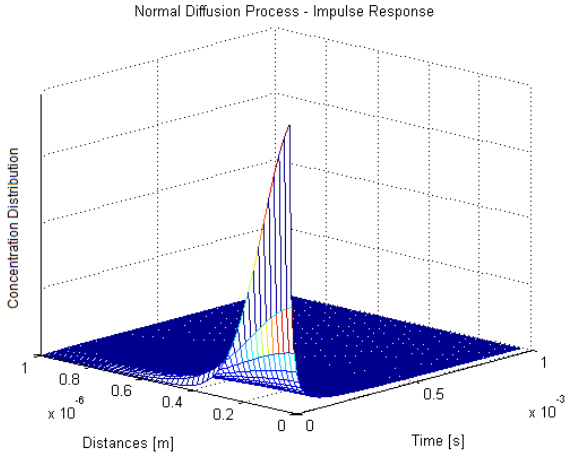

Figure 6: Normal diffusion scenario impulse response for a 3-D space and a transmission range of: 0–1 μm

The analytical solution to the second Fick's Law is shown next [17]:

$$C(r,t) = \frac{N}{(4\pi Dt)^{0.5n_{dim}}} e^{-\frac{r^2}{4Dt}} \tag{1}$$

where n_{dim} is the number of dimensions of the space, N is the total number of diffusing particles and D the diffusion constant.

Fig. 7 provides the result of the channel transfer function, showing the normalized gain and the group delay, both as functions of the transmission distance. The shown results are obtained for the same scenario as the impulse response analysis: calcium particles immersed in cytoplasm fluid in a 3-dimensional space and a transmission range of 0–1 μm.

The upper image and lower image in Fig. 7 show the normalized gain and the group delay, respectively. The channel presents, for any distance, a low pass filter behavior. This figure shows how attenuation increases with frequency and distance, and how the group delay increases with distance for the low frequency range.

7. Pulse Shaping

In a diffusion-based communication channel, simple modulation schemes are required, since the transmission of information requires the physical transportation of molecules, which is a slow process. According to this,

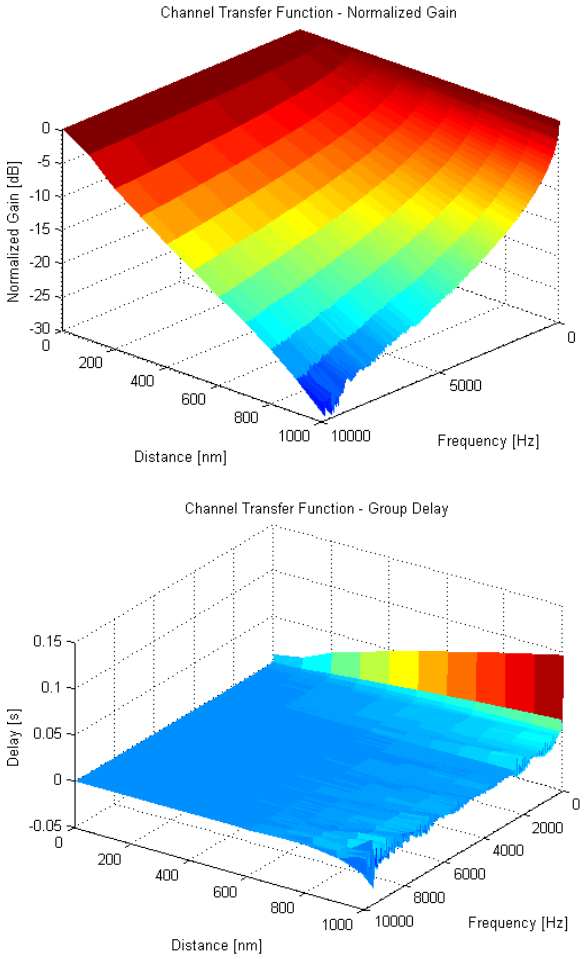

Figure 7: Normal diffusion scenario channel transfer function up to 10 kHz for a transmission range of 0–1μm: normalized gain (above) and group delay (below).

we propose to use a pulse-based modulation based on the exchange of concentration pulses due to their simplicity and bio-compatibility. Furthermore, pulse-based modulations present better results than carrier-based modulation techniques regarding energy management, which allows longer transmitting distances with a higher noise performance.

As it is mentioned in the previous section, the transmitted pulse shape is distorted due to the diffusion process. For any possible transmitted pulse shape, the receiver gets a pulse with a long tail that follows an exponential decay. The widening in reception of the transmitted pulses increases with the distance, and limits the maximum achievable bandwidth.

In the following, we simulate the transmission of different pulse shapes in order to find the optimal shape for pulse-based modulations. With the objective of testing the channel behavior for different input pulse shapes, we compare three different shapes: a square pulse, a cosine pulse, and a Gaussian pulse. We consider these shapes due to their differences in the frequency domain; for the same time duration, the Gaussian pulse has its frequency components concentrated around the low frequencies, the square pulse is the more widespread in frequency and the cosine pulse is in between.

We evaluate the suitability of each of these pulses by comparing the widening and the attenuation of the received signal for some distance values. The time duration and total energy of the transmitted pulses are fixed to a common value for all three pulse shapes.

Fig. 8 shows the transmission and reception of the three pulses, for a range of 400 nm. The green vertical lines correspond to the time instants when the received signal has the 50%, 60%, 70%, 80% and 90% of the total received energy, from left to right, respectively. We observe that all the received pulses have a long tail and they are therefore distorted, albeit with a different degree of distortion. The Gaussian pulse (in the third image) shows the least amount of distortion, while the square one (in the first image) is the most distorted one. The maximum peak level in reception is obtained for the Gaussian pulse. The vertical lines in Fig. 8 show that the energy distribution of the received pulses has almost no dependence on the pulse shape. In conclusion, for a pulse transmission constrained in its energy and in the time duration, the Gaussian shape yields to the best performance, even though the differences with other shapes are minimal.

The widening in the received pulse is distance-dependent. This width determines the maximum achievable bandwidth for this distance. A decrease in the width of the received pulse, and therefore an increase in the achievable

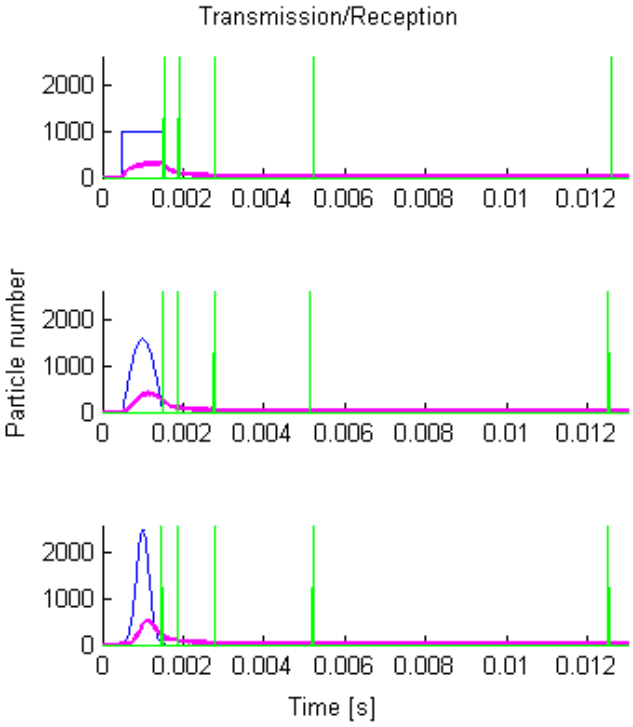

Figure 8: Square, cosine and Gaussian pulses transmission and its reception by a receiver located 400 nm away.

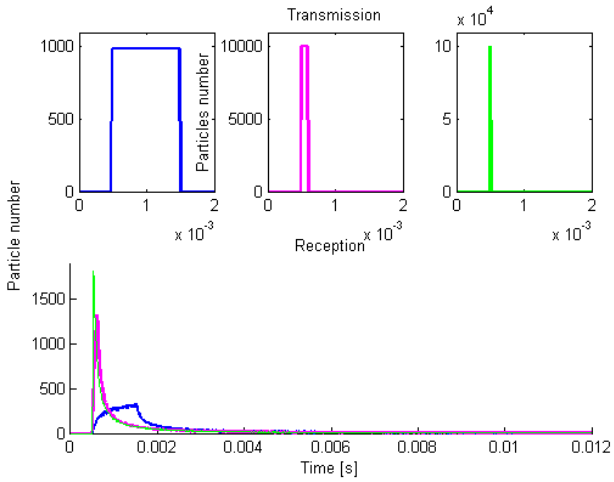

Figure 9: Transmission and reception of square pulses with the same energy and different time durations.

bandwidth, can be achieved by transmitting shorter pulses in time. Fig. 9 shows this effect. In the upper side of Fig. 9, the transmitted square pulses are shown, all of them with the same energy but having different lengths. The lower image shows the received pulses for the three transmissions; we observe that the minimum width corresponds to the case of transmitting the shortest square pulse.

After this analysis, we conclude that: i) the optimal pulse shape is a spike, a very narrow pulse, which gives the lowest pulse width at the receiver and thus the highest achievable bandwidth, and ii) the shape of the transmitted pulses is not important, since the total energy received is not shape dependent.

8. Evaluation of Pulse-based Modulation Techniques

Communication of larger amounts of information can be achieved by transmitting a train of pulses (spikes), and by changing one or more of their parameters. In this section, we evaluate four modulation techniques for trains of pulses, namely, Pulse Amplitude Modulation (PAM), Pulse Position Modulation (PPM), Communication trough Silence (CtS) and Rate Modulation (RM).

As any transmitted signal suffers a time widening dependent on the dis-

tance between the transmitter and the receiver, in order to avoid Inter-Symbol Interference (ISI), which can create undecodable sequences at the receiver side, a guard time between symbols is added in transmission. The *symbol time*, T_s, is the sum of the symbol duration and the guard time. A trade-off between increasing the rate while increasing ISI in reception must be reached by adjusting the guard time in transmission.

We compare the four modulation schemes by considering the received concentration when the following reference bit stream is transmitted: "0110110001". This bit stream is encoded as a sequence of concentration pulses with a constrain in the total transmission time, equal to T_{seq}=0.03 s, and in the total number of transmitted particles.

We consider a particular case of the binary PAM modulation known as On-Off Keying (OOK). In this modulation, a logical "1" is transmitted by sending a spike at the beginning of the *symbol time*, and a logical "0" is transmitted as silence. This scheme is compared with a binary PPM modulation, which requires to divide the *symbol time* in two halves, and codifies a logical "1" by transmitting a spike during the first half of the *symbol time*, and a logical "0" by transmitting a spike during the second half.

We also evaluate a modulation scheme known as Communication through Silence (CtS), which uses time as a new dimension to encode the information. A transmission of a first spike is needed as a preamble bit (start pulse), and a last spike is needed in order to finish the transmission (stop pulse). The symbol is encoded into the time between both pulses; thus, the *symbol time* is variable. This communication scheme requires synchronization, i.e., receiver and transmitter must share a common clock. In our analysis, both for CtS and RM, we consider the particular case of a 32-symbol modulation (five bits per symbol). Therefore, the previous bit stream is encoded as a sequence of two symbols "13, 17" and it is compared to the 32-symbol modulation version of Rate Modulation scheme.

In the Rate Modulation scheme, the *symbol time* is fixed and information is encoded into the rate of transmission of spikes. For instance, in this analysis, the transmission rate for symbol "17" is higher than the rate for symbol "13". The receiver nanomachine will sense the concentration and will decode the transmitted symbol by counting the mean number of pulses within the *symbol time*. A priori, this modulation scheme appears to be highly inefficient in terms of energy, since it is based on transmitting a train of spikes per symbol. In consequence, the maximum achievable bandwidth will predictably be lower than with the other commented schemes. However,

	$P - P_{meanvalue}$	$P_{max}[Particlesnumber]$
OOK	9.65	1136
PPM	7.89	591
CtS	76.37	3615
RM	2.84	471

Table 1: Evaluation metrics comparison for OOK, PPM, CtS and RM schemes.

since it is widely used for communication in the nervous system, it seems the most bio-compatible technique.

The four modulation schemes are analyzed and their performance over the diffusion-based MC channel is compared regarding the ISI for a specific rate of transmission and the transmission range for a limited transmitted power. The Peak to Peak Value ($P - P$) and the Maximum Value (P_{max}) are used as the evaluation metrics.

In order to compare the four modulations under the same conditions, constraints are set in the overall energy (energy per sequence, E_{seq}) and in the total transmission time (sequence duration T_{seq}). In this analysis, $E_{seq} = 1^6$ particles, which corresponds to 100.000 particles per pulse in OOK, 50.000 particles per pulse in PPM, 333.333 particles per pulse in CtS and 33.333 particles per pulse in RM, and a $T_{seq} = 0.03s$.

Fig. 10 (a) shows the transmitted concentration sequences according to each scheme (OOK, PPM, CtS and RM respectively). Fig. 10 (b) shows the reception process for the four transmissions at a distance of 500 nm. The vertical green lines show the *symbol time* for each modulation scheme and the red data the decoded information sequence the receiver recovers.

In order to compare the performance of the different modulation schemes in Fig. 11 the four receiving processes for a distance of 500 nm are shown superimposed. Table 1 shows the obtained results for this analysis. In the first column, the mean Peak to Peak values are shown as Inter-Symbol-Interference metric; in the second column, the mean Maximum Values are shown as the transmission range metric. The results show how for both ISI and transmission range the best performance is expected with the CtS modulation scheme, followed by the OOK, PPM and the worst performance correspondes to the RM scheme.

CtS outperforms the other modulation schemes since the average number of transmitted pulses is lower than the number of pulses for the rest of modu-

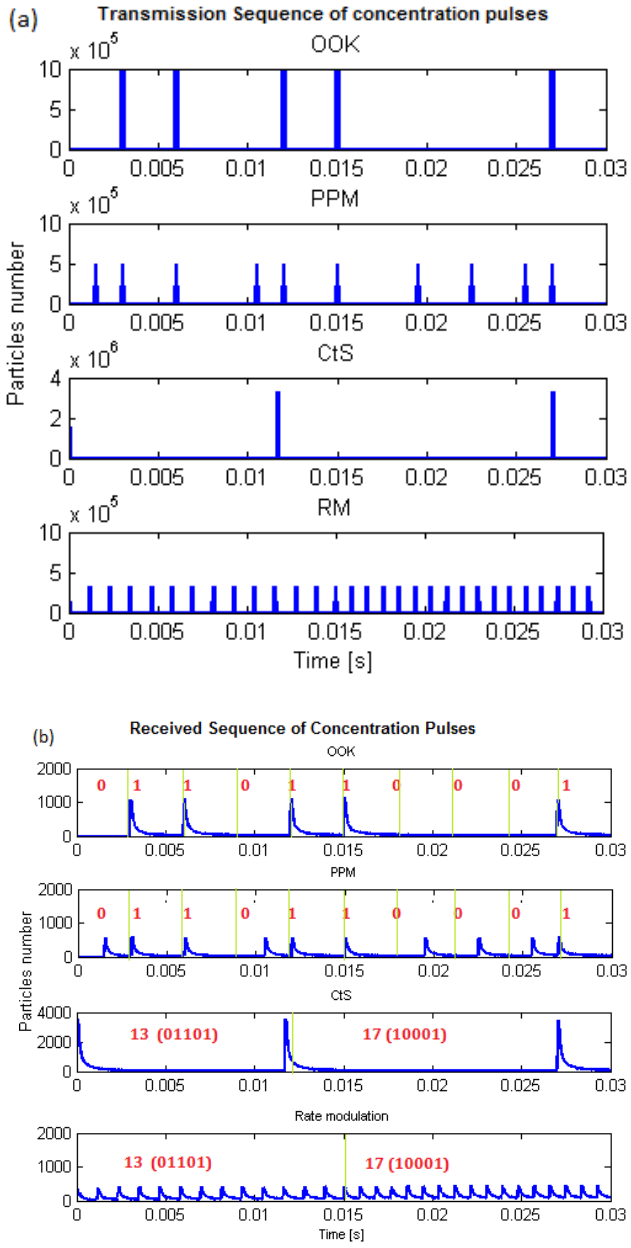

Figure 10: (a) Transmission process for OOK, PPM, CtS and RM. (b) Reception process for OOK, PPM, CtS and RM for a distance of 500 nm.

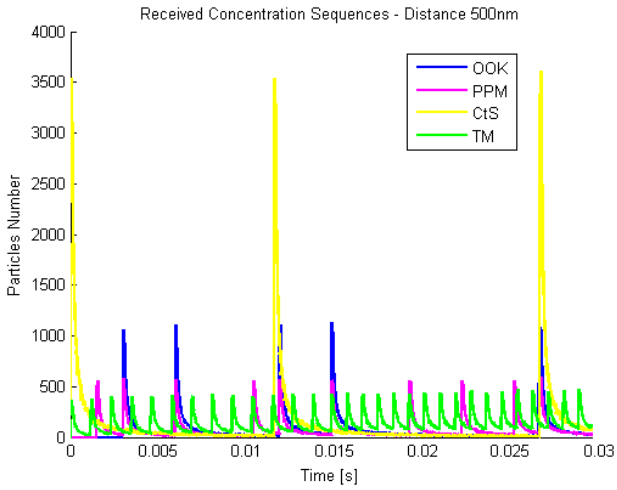

Figure 11: Reception process for OOK, PPM, CtS and RM modulation schemes for a transmission distance of 500 nm.

lation schemes. As a consequence, the transmitter can encode the CtS pulses using more energy than with RM, OOK or PPM, and CtS pulses reach the receiver with the highest power and they are easier to decode.

However, biological nanomachines are expected to be simple machines with limited computing capabilities, hence, as we mentioned in Section 7, simplicity is one of the most important factors when choosing the most suitable modulation scheme for diffusion-based MC. Therefore, we disregard CtS, since it requires perfect synchronization between the transmitter and the receiver nanomachines in order to properly decode the transmitted signal. OOK appears to be the simplest modulation scheme, since it does not require synchronization and the decoding is based in comparing the sensed concentration with a concentration threshold which says if the transmitted symbol was a logical "0" or a logical "1". Moreover, since with OOK one of the symbols is transmitted as a silence, the ISI is reduced and its maximum value is higher than with PPM or RM.

To summarize, the results obtained by simulation point to PAM (OOK) as the most suitable modulation scheme to be used in the diffusion-based communication channel, in terms of simplicity (no overhead for synchronization), throughput, energy management and ISI.

9. Conclusions

In this work, we detail different diffusion-based scenarios that can be simulated through *N3Sim* according different assumptions on the physical layer. We have proved the linearity and temporal invariance of the diffusion-based MC channel in the case of free diffusion, by simulating the motion of each particle with Brownian dynamics as well as by including elastic collisions as interactions. We have validated the diffusion-noise when the receiver estimates the concentration by counting the number of molecules in its sensing area, with the Particle Counting Noise model from [21].

After a pulse shaping analysis, we conclude that, the transmission of the shortest possible pulses is needed to reach a given distance range while having the maximum possible bandwidth available. Ideally, the optimal pulse shape is a spike of particles with zero length. The total transmitted energy for a symbol determines its transmission range, and this does not depend on the shape of the pulse. After the comparison of four pulse-based communication schemes, we conclude that OOK is the most efficient binary modulation scheme for the diffusion-based MC channel.

We believe that the future work on this topic can take advantage from the results presented in this paper. In particular, these results point out that in a molecular nanonetwork, in order to minimize the overall energy consumption while allowing for a correct reception of the transmitted signal, the transmitter nanomachines should be able to adjust the energy and the duration of the transmitter pulses. While this can be in contrast with the basic capabilities expected by the nanomachines, we believe that a series of suboptimal schemes can be studied in order to meet possible performance limitations.

Acknowledgment

This work has been partially supported by the FPU grant of the Spanish Ministry of Education.

References

[1] Akyildiz IF, Brunetti F, Blàzquez C. Nanonetworks: A new communication paradigm. Computer Networks 2008;52(12):2260 –79.

[2] Moore M, Enomoto A, Nakano T, Egashira R, Suda T, Kayasuga A, et al. A Design of a Molecular Communication System for Nanomachines Using Molecular Motors. IEEE International Conference on Pervasive Computing and Communications 2006;.

[3] Liu JQ, Nakano T. An information theoretic model of molecular communication based on cellular signaling. In: 1st International ICST Workshop on Computing and Communications from Biological Systems: Theory and Applications. ICST; 2007,.

[4] Nakano T, Suda T, Moore M, Egashira R, Enomoto A, Arima K. Molecular communication for nanomachines using intercellular calcium signaling. In: Fifth IEEE Conference on Nanotechnology. 2005, p. 632–5.

[5] Gregori M, Akyildiz IF. A new nanonetwork architecture using flagellated bacteria and catalytic nanomotors. IEEE JSel A Commun 2010;28(4):612–9.

[6] Parcerisa L, Akyildiz IF. Molecular Communication Options for Long Range Nanonetworks. Computer Networks 2009;53(16):2753–66.

[7] Pierobon M, Akyildiz IF. A physical End to End Model for Molecular Communication in Nanonetworks. Journal of Selected Areas in Communications (JSAC) 2010;28(4):602–11.

[8] Silva GA. Introduction to nanotechnology and its applications to medicine. Surgical Neurology 2004;61:216 –20.

[9] Freitas RA. Nanotechnology, nanomedicine and nanosurgery. International Journal of Surgery 2005;3(4):243–6.

[10] Malsch I. Biomedical applications of nanotechnology. In: The Industrial Physicist. 2002, p. 15–7.

[11] Pierobon M, Akyildiz IF. Information capacity of diffusion-based molecular communication in nanonetworks. In: Proc. IEEE Infocom Miniconference. 2011,.

[12] Atakan B, Akan OB. Deterministic capacity of information flow in molecular nanonetworks. Nano Communication Networks (Elsevier) 2010;.

[13] Atakan B, Akan OB. On Channel Capacity and Error Compensation in Molecular Communication. Springer Transactions on Computational Systems Biology 2008;10:59–80.

[14] Kadloor S. Adve R. A framework to study the molecular communication system. In: Internatonal Conference on Computer Communications and Networks. 2009,.

[15] Gul E, Akan OB. NanoNS: A Nanoscale Network Simulator Framework for Molecular Communications. Nano Communication Networks (Elsevier) 2010;1(2):138–56.

[16] Philibert J. One and a half century of diffusion: Fick, einstein, before and beyond. Diffusion Fundamentals 2005;:1.1–1.10.

[17] Ursell TS. The Diffusion Equation A Multi-dimensional Tutorial. 2007.

[18] Ermak DL, Mccammon JA. Brownian dynamics with hydrodynamic interactions. J Chem Phys 1978;69:1352–60.

[19] Vlahos L, Isliker H, Kominis Y, Hizanidis K. Normal and Anomalous Diffusion: A Tutorial. 2008.

[20] Mendez V, Fedotov S, Horsthemke W. Reaction-Transport Systems: Mesoscopic Foundations, Fronts, and Spatial Instabilities. Springer; 2010.

[21] Pierobon M, Akyildiz IF. Diffusion-based Noise Analysis for Molecular Communication in Nanonetworks. IEEE Transactions on Signal Processing 2011;59(6):2532–47.

[22] Surhone L, Timpledon M, Marseken S. Superposition Principle: Physics, Systems Theory, Linear System, Linear, Linear Map, Algebraic Equation, Linear Differential Equation, Simultaneous Equations, Vector Field, Euclidean Vector. Betascript Publishers; 2010.

[23] Llatser I, Alarcón E, Pierobon M. Diffusion-based Channel Characterization in Molecular Nanonetworks. In: IEEE International Workshop on Molecular and Nanoscale Communications (MoNaCom). 2011, p. 467–72.